



Scholars Research Library

Der Pharmacia Lettre, 2014, 6 (6):289-296
(<http://scholarsresearchlibrary.com/archive.html>)



3D-QSAR and molecular docking studies of quinazoline derivatives as glycogen synthase kinase-3 β (Gsk-3 β) inhibitors

Srinivas Sangu^{1*}, Aparna Vema² and Rajkamal Bigala¹

¹Department of Pharmaceutical Chemistry, Ganga Pharmacy College, Das Nagar, Nizamabad, T.S, India

²Department of Pharmaceutical Chemistry, Sree Chaithanya Institute of Pharmaceutical Sciences, LMD Colony, Karimnagar, T.S, India

ABSTRACT

The discovery of glycogen synthase kinase-3 β (GSK3 β) inhibitors has proven to be a challenging task to identify novel and potent gsk3 β inhibitors. The quantitative structure activity relationship (QSAR) and docking approach became very useful and largely widespread technique for ligand-based drug design. The computational study deals with development of 3D QSAR models for 85 selected quinazoline derivatives using the stepwise variable selection k-nearest neighbor molecular field analysis approach; a leave-one-out cross validation method. The developed model showed satisfactory statistical significance r^2 (Regression) with 0.75 and q^2 (Correlation coefficient) 0.81. Further we have carried out molecular docking studies with the x-ray crystal structure of glycogen synthase kinase domain. These studies showed that quinazoline scaffold can be utilized for designing of novel GSK-3 β inhibitors.

Key words: GSK-3 β inhibitors, Quinazoline derivatives, Docking studies and QSAR studies.

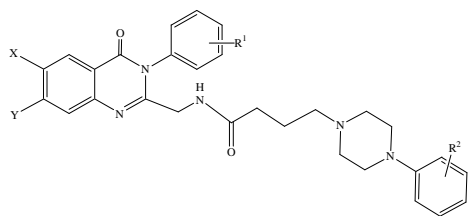
INTRODUCTION

The glycogen synthase kinase3 β was originally identified and studied for its functions in the regulation of glycogen synthase as the rate limiting enzyme in glycogen biosynthesis [1]. It is serine /threonine kinase comprising two isoforms (α and β) in mammals. These isoforms share high homology (>90%) at the catalytic domain and expressed ubiquitously in cellular system and have similar biochemical properties [2]. GSK3 β has multiple substrates and plays a critical role in glucose homeostasis, CNS function [3], circadian rhythm, controlling cell cycle, neuro degeneration, chronic inflammatory diseases and cancer [4-5]. The literature reveals that the maleimides of inhibitors (bisaryl maleimides) [4], anilino maleimides [5], bisindolyl maleimides [6], azaindolyl maleimides [7-9] have been reported to show a degree of selectivity toward GSK3 β . Although, a number of diverse classes of GSK3 β inhibitor have been reported so far, the selectivity problem appears to hamper all efforts. This at least in part, stems from the fact that the kinase has the same natural substrates, ATP and most of the ligands act through competition with ATP. This calls for methodologies that tackle the non selectivity to address the design of potential drug candidates of GSK3 β inhibitors. In the present study the quinazoline derivatives were (85) selected to develop the 3D-QSAR and molecular docking studies.

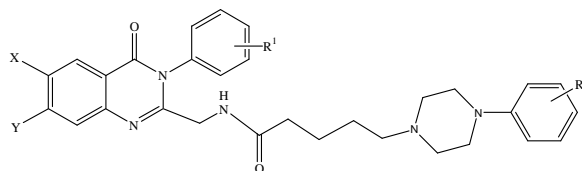
MATERIALS AND METHODS

Synthesis of molecules:

All molecules (85) under study were taken from previously published work and IC₅₀ (nM) values converted in to – log₁₀ (pIC₅₀) values used in the present study were shown in Table1.[10]



Compound 1-19



Compound 20-85

Table1 Showing the compounds under present study

Compound	X	Y	R ¹	R ²	Activity (pIC ₅₀)
1	H	H	H	H	6.02
2	H	H	H	o-Cl	6.29
3	H	H	H	p-Cl	6.43
4	H	H	H	p-Me	6.13
5	H	H	H	2,3-Me ₂	7.02
6	H	H	H	2,4-Me ₂	6.19
7	H	H	H	3,4-Me ₂	5.95
8	H	H	H	o-OMe	7.09
9	H	H	H	m-OMe	5.58
10	H	H	H	p-OMe	6.14
11	H	H	H	o-OEt	7.34
12	H	H	H	p-NO ₂	5
13	H	H	H	p-Ac	6.02
14	H	H	p-F	H	6.16
15	H	H	p-F	2,4-Me ₂	6.3
16	H	H	p-F	2,6-Me ₂	6.3
17	H	H	p-F	p-OMe	5.6
18	H	H	p-F	o-OEt	5.88
19	H	H	p-F	p-NO ₂	5.13
20	H	H	H	H	6.18
21	H	H	H	o-F	6.39
22	H	H	H	p-F	5.61
23	H	H	H	o-Cl	6.88
24	H	H	H	m-Cl	6.95
25	H	H	H	p-Cl	6.34
26	H	H	H	3,4-Cl ₂	6.79
27	H	H	H	2,3-Me ₂	6.33
28	H	H	H	2,4-Me ₂	6.16
29	H	H	H	2,5-Me ₂	6.37
30	H	H	H	3,4-Me ₂	6.69
31	H	H	H	o-OMe	7.67
32	H	H	H	m-OMe	5
33	H	H	H	p-OMe	5.69
34	H	H	H	o-OEt	7.58
35	H	H	H	m-CF ₃	6.45
36	H	H	H	p-Ac	5
37	H	F	H	H	6.03
38	H	F	H	o-F	6.11
39	H	F	H	p-F	6.11
40	H	F	H	o-Cl	7.28
41	H	F	H	m-Cl	6.72
42	H	F	H	p-Cl	5.65
43	H	F	H	3,4-Cl ₂	6.34
44	H	F	H	2,3-Me ₂	7.12
45	H	F	H	2,4-Me ₂	6.02
46	H	F	H	2,5-Me ₂	5.82

47	H	F	H	3,4-Me ₂	6.22
48	H	F	H	o-OMe	7.07
49	H	F	H	m-OMe	5
50	H	F	H	p-OMe	5.95
51	H	F	H	o-OEt	7.72
52	H	F	H	m-CF ₃	7.03
53	H	F	H	p-Ac	6.16
54	F	H	H	H	6.32
55	F	H	H	o-F	6
56	F	H	H	p-F	6.37
57	F	H	H	o-Cl	6.69
58	F	H	H	m-Cl	6.88
59	F	H	H	p-Cl	5.92
60	F	H	H	3,4-Cl ₂	6.56
61	F	H	H	2,3-Me ₂	7.25
62	F	H	H	2,4-Me ₂	6.2
63	F	H	H	2,5-Me ₂	6.69
64	F	H	H	3,4-Me ₂	6.58
65	F	H	H	o-OMe	6.92
66	F	H	H	m-OMe	6.03
67	F	H	H	p-OMe	6.45
68	F	H	H	o-OEt	7.92
69	F	H	H	m-CF ₃	7.13
70	F	H	H	p-Ac	6.22
71	H	H	o-OMe	o-OMe	6.67
72	H	H	o-OMe	o-OEt	7.53
73	H	F	o-OMe	o-OEt	6.95
74	F	H	o-OMe	o-OMe	7.1
75	F	H	o-OMe	o-OEt	7.31
76	H	H	m-OMe	o-OMe	7
77	H	H	m-OMe	o-OEt	7.25
78	H	F	m-OMe	o-OEt	7.04
79	F	H	m-OMe	o-OMe	6.63
80	F	H	m-OMe	o-OEt	7.79
81	H	H	p-OMe	o-OMe	7.01
82	H	H	p-OMe	o-OEt	7.53
83	H	F	p-OMe	o-OEt	7.3
84	F	H	p-OMe	o-OMe	6.72
85	F	H	p-OMe	o-OEt	7.79

3D-QSAR studies:

The molecular modeling and docking studies (3D & Docking) were performed using the molecular Design suite (VLife MDS software package, version 4.3; from VLife sciences, pune, India). The structures of all compounds were sketched in chem sketch version 12.0 (ACD lab). All structures are cleaned and 3D optimized. Energy minimization and geometric optimization were conducted using the Merck molecular force field (MMFF) and Gasteiger marsili charges for the atoms with the root mean square gradient set to 0.01kal/mol A⁰ and the iteration limit to 10,000. The conformers for all structures are generated and the low energy conformer was selected for each compound for further study.

Data set and Molecular modeling for 3D-QSAR:

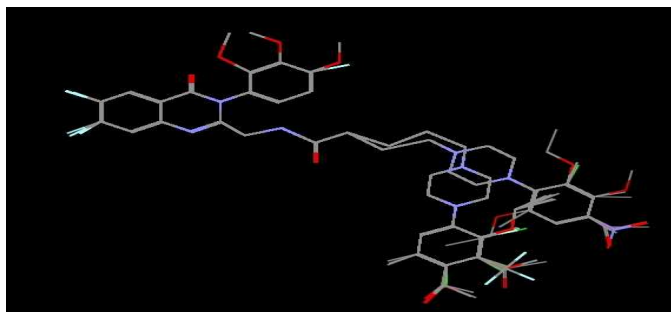
The total set of compounds was divided in to training set (58 molecules) for generating 3D-QSARmodel and test set (27 molecules) for validating the quality of the models. Optimal training and test set were generated using the sphere exclusion (SE) algorithm. The SE method was adopted for division of training and test data set comprising of (58 molecules) and (27 molecules) molecules respectively, with dissimilarity value of 5.0 where the dissimilarity value gives the SE radius.

Alignment procedure:

Molecular alignment is a crucial step in 3D-QSAR study to obtain meaningful results. Energy minimized and geometry optimized structure of each molecule were aligned by the template based method. In general geometric similarity should exist between the modeled structure and the bioactive conformation for 3D-QSAR. This special alignment of compounds under study is thus one of the most sensitive and determining factor in obtaining a reliable model. Alignment of all 85 compounds was done using the template based alignment by using the most active

molecule as reference and (4-oxo-3, 4 dehydro-2yl-3phenyl-quinazoline derivative) as template in MDS; the alignment of all compounds in present study shown in Fig 1. The aligned structures were used for the study. In the template alignment, a template structure was defined and used as a basic for alignment of a set of molecules. These aligned conformations were used to generate the predictive QSAR model.

Fig1. Figure showing alignment of molecules used in the study.



Descriptor calculation:

In this study by using Tripos force field (11) and Gasteiger –marsili charges (12) electrostatic and steric descriptors were calculated. The dielectric constant was set to 1.0 considering the distance-dependent dielectric function probe setting was carbon atom with charge ± 1.0 . This resulted in calculation of 5,000 field descriptors (1,680 for each electrostatic and steric) for all the compounds. QSAR analysis was performed after removal of all the invariable descriptors, as they do not contribute to the QSAR.

3D-QSAR studies were carried out by kNN method using forward step wise variable selection as variable selection method. The kNN methodology relies on a simple distance learning approach where by an unknown member is classified according to the majority of its kNN in the training set. The nearness is measured by an appropriate distance metrics (a molecular similarity measure calculated using field interactions of molecular structures). The step-by-step search procedure beings by developing a trial model with a single dependent variable and independent variable, one step at a time, examining the fit of model at each step (using weighted kNN cross-validation procedure). The method continues until there is no more significant variable remaining outside the model. Once the training and test sets are generated, kNN methodology is applied to the descriptors generated over the grid. The steric, electrostatic, and hydrophobic energies are computed at the lattice points of the gride using a methyl probe of charge ± 1 . These interaction energy values are considered for relationship generation and utilized as descriptors to decide the nearness between molecules. k-nearest neighbor molecular field analysis (kNN-MFA) model were developed using the Forward stepwise variable selection method with cross-correlation limit set of 5.0 and term selection criteria as r^2 . F-test was set to 4.0. As some additional parameters, variance cutoff was set at 0.000 kcal/mole Å and scaling to none; additionally, kNN parameter setting was done within the range of 2-5 and the prediction was selected as the distance based weighted average. To systematically assess a QSAR model, a reliable validation is required usually; a QSAR model is evaluated by the predictive results for the given dataset. The models having r^2 (0.75) were checked for their external predictivity.

Docking studies:

The docking studies helped to sort-out the designed compounds with good binding affinity against glycogen synthase kinase enzyme. We conducted docking studies using Biopredicta module of VLife MDS 4.3 using crystal structure of the glycogen synthase kinase retrieved from protein data bank (PDB Id.4ACC).

RESULTS AND DISCUSSION

The computational study deals with development of 3D QSAR for 85 selected quinazoline derivatives using the stepwise variable selection k-nearest neighbour molecular field analysis approach; a leave-one-out cross validation method. The developed model showed satisfactory statistically significant r^2 (Regression) with 0.75 and q^2 (Correlation coefficient) 0.81 were shown in Table 2. Further molecular docking studies were carried out with the x-ray crystal structure of glycogen synthase kinase domain and the dock scores (kcal/moles) of all compounds were shown in Table 3.

Table2. Showing the selected QSAR model along with statistical parameters employed for the model selection

Descriptor Range	k Nearest Neighbour	N	q ²	q ² _se	pred_r ²	pred_r ² se
E_1444 (4.0362 4.1324)	2	58	0.8172	0.7236	0.7575	0.5150
E_1579 (0.9146 0.9899)						
S_472(4.8157 5.0486)						

Table3. Showing the Actual, predicted activities along with residuals and Docking scores of quinazoline derivatives using SW-kNN MFA method

Sl.No.	Actual activity	Predicted activity (pIC50)	Residuals	Docking score
1	6.02	6.044	-0.34	-3.190149
2	6.29	6.093	-0.34	-4.01869
3	6.43	5.852	-0.34	-4.611467
4	6.13	5.95	-0.34	-3.048052
5	7.02	6.175	-0.34	-4.395815
6	6.19	6.09	-0.34	-4.285131
7	5.95	6.09	-0.34	-4.204618
8	7.09	7.329	-0.34	-4.124801
9	5.58	6.073	-0.34	-4.080334
10	6.14	5.798	-0.34	-4.522176
11	7.34	7.085	-0.34	-3.892629
12	5	5.242	-0.34	-4.028881
13	6.02	5.888	-0.34	-4.304687
14	6.16	6.091	-0.34	-1.403753
15	6.3	6.244	-0.34	-3.557473
16	6.3	6.178	-0.34	-4.229233
17	5.6	6.088	-0.34	-4.086438
18	5.88	6.085	-0.34	-3.092155
19	5.13	5.151	-0.34	-4.39268
20	6.18	6.238	-0.34	-3.747464
21	6.39	6.056	-0.34	-4.409298
22	5.61	5.57	-0.34	-4.260995
23	6.88	6.86	-0.34	-3.236679
24	6.95	6.739	-0.34	-3.201721
25	6.34	5.669	-0.34	-1.450164
26	6.79	6.253	-0.34	-3.115317
27	6.33	6.305	-0.34	-4.205425
28	6.16	6.232	-0.34	-3.982151
29	6.37	6.305	-0.34	-3.94702
30	6.69	6.17	-0.34	-3.957804
31	7.67	7.301	-0.34	-2.427283
32	5	5.304	-0.34	-1.935696
33	5.69	5.805	-0.34	-2.764349
34	7.58	7.722	-0.34	-4.298745
35	6.45	6.99	-0.34	-2.233518
36	5	5.512	-0.34	-3.448983
37	6.03	6.524	-0.351	-3.763191
38	6.11	6.172	-0.351	-2.155975
39	6.11	6.25	-0.351	-4.054487
40	7.28	6.632	-0.351	-4.242139
41	6.72	6.341	-0.351	-2.925613
42	5.65	6.028	-0.351	-1.953481
43	6.34	6.482	-0.351	-3.956572
44	7.12	6.524	-0.351	-2.21275
45	6.02	6.552	-0.351	-4.00793
46	5.82	6.524	-0.351	-3.587913
47	6.22	6.524	-0.351	-3.902675
48	7.07	7.148	-0.351	-2.493879
49	5	5.299	-0.351	-3.416451
50	5.95	6.004	-0.351	-3.66064
51	7.72	7.275	-0.351	-2.218624
52	7.03	6.702	-0.351	-3.643802
53	6.16	5.976	-0.351	-2.501931
54	6.32	6.17	-0.387	-3.912165
55	6	6.232	-0.387	-2.423559
56	6.37	6.125	-0.387	-3.989039
57	6.69	6.16	-0.387	-4.202147

58	6.88	7.19	-0.387	-4.066853
59	5.92	6.081	-0.387	-4.186153
60	6.56	6.335	-0.387	-4.417856
61	7.25	6.785	-0.387	-2.815035
62	6.2	6.97	-0.387	-3.170191
63	6.69	7.067	-0.387	-3.871213
64	6.58	6.505	-0.387	-3.948909
65	6.92	7	-0.387	-3.662417
66	6.03	5.627	-0.387	-3.85669
67	6.45	5.808	-0.387	-2.772099
68	7.92	7.684	-0.387	-3.440656
69	7.13	6.786	-0.387	-4.188419
70	6.22	5.826	-0.387	-3.982536
71	6.67	7.242	-0.371	-1.897574
72	7.53	7.247	-0.371	-3.975201
73	6.95	7.553	-0.379	-1.844738
74	7.1	7.417	-0.418	-2.223641
75	7.31	7.241	-0.418	-3.610979
76	7	7.159	-0.35	-3.67952
77	7.25	7.268	-0.35	-3.752281
78	7.04	7.273	-0.359	-3.896853
79	6.63	7.851	-0.399	-2.412773
80	7.79	7.854	-0.399	-3.754813
81	7.01	7.3	-0.342	-1.888118
82	7.53	7.277	-0.342	-1.762175
83	7.3	7.303	-0.351	-2.987971
84	6.72	7.79	-0.392	-1.121769
85	7.79	7.849	-0.392	-2.161401

Interpretation of QSAR model:

In the present study several 3D-QSAR models were generated using stepwise variable selection method. Of the several statistically significant models best model is reported here in Table 2. 3D-QSAR model was selected based on the values of statistical parameters and the best kNN-MFA 3D-QSAR models with (58) training set compounds having a q^2 0.81 and pre_r^2 0.75. The kNN-MFA QSAR method explores formally the active analog approach which implies that compounds display similar profiles of pharmacological activities. In this method, the activity of each compound is predicted as average activity of most chemically similar compound from the data set. The predictive ability of this forward step wise variable selection kNN-MFA model was evaluated by predicting the biological activities of the test set molecules. Residual values obtained by subtracting of predicted activities from biological activities were found near to zero. Therefore it was concluded that the resultant QSAR model have good predictive ability. The actual, predicted activities and residuals of both training and test set molecules are given Table 3. The contribution plot and fitness plot of observed verses predicted activity of both training and test set molecules helped in cross validation of kNN-MFA QSAR model are depicted in Fig 2 & Fig 3. The model selection criterion is based on the value of q^2 , the internal predictive ability of the model and that of $pred_r^2$, the ability of the model to predict the activity of external test set. The selected model was found to be statistically most significant, especially with respect to the internal predictive ability q^2 (0.81) of the model. The correlation coefficient suggests that our model is reliable and accurate. A data set of (27) compounds were selected as the test set from the original data of 85 compounds for the cross validation. The predicted versus the experimental values for the training and test sets are depicted in Fig 4. The values of $pred_r^2$ for the test set with value of (0.75), which means better predictive power for the external test set. Thus our model displays good predictivity in regular cross validation.

In 3D-QSAR studies the steric and electro static fields were calculated using Tripos force field and Gasteiger-marsili charges, 3D data points were generated. The range of property values in the generated data point helped for the design of new chemical entities. These ranges were based on the variation of the field values at the choosen points using the most active molecule and its nearest neighbor set. The points generated is SW-kNN-MFA 3D QSAR model are S_472 (4.8157, 5.0486), E_1444 (4.0362, 4.1324) and E_1579 (0.9146, 0.9849) that is steric and electrostatic interaction fields at lattice points 472, 1444 and 1579 respectively as shown in Fig 5. These points suggested the significance and requirement of steric and electrostatic properties as mentioned in the range in parenthesis for structure activity relationship (SAR) and maximum biological activities of quinazoline analogues. The steric interaction fields are represented in green lattice point at S472 implies that steric interaction along these lattice points are required to be addressed and interaction at this point S472 are positively contributing are so the compounds which are having bulky substituent at aromatic ring can show the increased activity. The two

electrostatic fields at blue lattice point at E1444 and E1579 implies that electronegative group are positively contributing so the compound which are having electron withdrawing group i.e. ortho methoxy and ortho ethoxy group at R² position can show the increased activity of compounds. The m-Chloro group and p-Chloro group can contribute the more biological activity than ortho floro and para floro groups.

Fig2. Contribution plot for descriptors in QSAR model

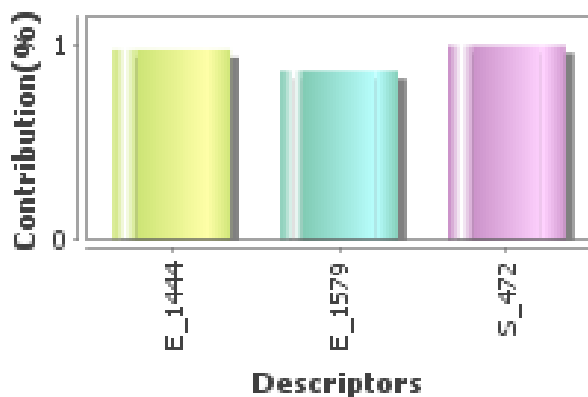


Fig 3. Fitness plot of Actual versus Predicted activity of training (red) and Test (blue) set compounds.

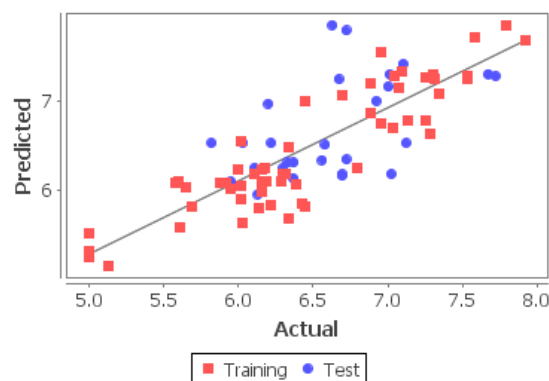


Fig4. Figures showing the Actual (red) and predicted activity (blue) of test and training set compounds

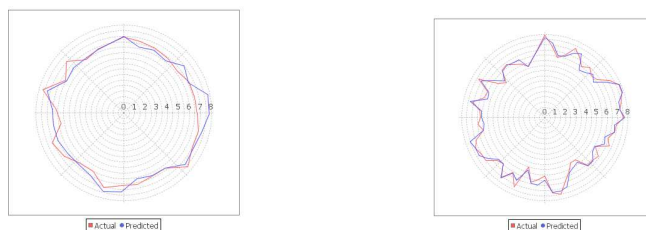
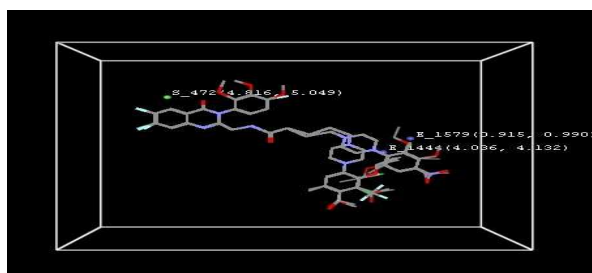


Fig5. Figure showing the field points used in the QSAR model

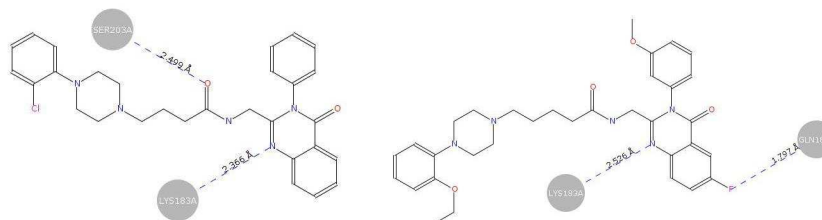


Docking results:

To gain insight in to the molecular determinants that modulate the inhibitory activity of these compounds, molecular docking simulations for these compounds to GSK3 β were performed using the biopredicta program in VLife MDS software based on the x-ray crystal structure of GSK3 β was retrieved from protein data bank (pdb id. 4ACC). The docking and subsequent scoring were performed using the default parameters of the biopredicta program demonstrated that all the molecules under study have a nice interaction with amino acids of GSK3 β , and all the compounds with ortho ethoxy, ortho methoxy groups shown to exhibit good binding interaction and elucidate the good docking score, the para Chloro and meta Chloro groups shows the good docking score than ortho floro and para floro groups. The dock scores (kcal/moles) of all compounds were shown in Table 3. The nitrogen atom of quinazoline ring forms hydrogen bonding with **LYS183** with a 2.366 Å distance. The oxygen atom of keto group interacts with **SER203** with 2.499 Å distance (compound 2). The electron withdrawing group (fluorine) substituted on phenyl ring at para position can form a hydrogen bonding with **LYS183** (2.526 Å distance) and **GLN185** with

1.797 Å distance (compound 80). The oxygen atom of amide group forms hydrogen bonding with SER 203 with a 2.059 Å distance and the oxygen atom of methoxy group interact with ARG96 with a 2.48 Å distance (compound 84). The most active molecule (2 and 80) interaction images depicted in Fig 6.

Fig6. Figure showing the hydrogen bonding of compound 2 and 80 with active sites gsk3 (pdb id. 4acc)



CONCLUSION

In conclusion a computational approach along with the QSAR and docking analysis was employed to identify molecular structural features, electrostatic and steric effect dominantly determine binding affinities which can be useful for development of glycogen synthase kinase inhibitors.

Acknowledgment

Authors are thankful to the Ganga Educational Society for providing the facilities. The authors have declared no conflict of interest.

REFERENCES

- [1] S. Lan, P. Catherine, R.C. Bruce, W. Lori, Z.X. Jun, A.L. Richard, B. Mary pat, R.Jerry, VM. William, K T .Demarest, K .Gee-Hong, *Bioorg Med Chem*, **2004**, 12, 1239-1255.
- [2] J. O. David, S. Lan, P. Catherine, R.C. Bruce, W. Lori, Z.X. Jun, Z .Han-Cheng, V M. William, K T. Demarest, K. Gee-Hong, E M. Bruce, *Bioorg Med Chem*, **2004**, 12, 3167-3185.
- [3] K. Conrad, L. Kathrin, L. Maryse, M. Laurent, L. Thomas, *Bioorg Med Chem Lett*, **2004**, 14, 413-416.
- [4] T A. Engler, S. Malhotra, T P. Burkholder, JR. Henry, D. Mendel, W J. Porter, K. Furness, C. Diefenbacher, A. Marquart, *Med Chem Lett*, **2005**, 15, 899-903.
- [5] D.G. Smith, M. Buffet, A.E. Fenwick, D. Haigh, M. Saunders, R. Stacey, RW. Ward, *Bioorg Med Chem Lett*, **2001**, 11, 635-639.
- [6] Z. Hang-Cheng, B.W. Kimberly, Y. Hong et al., *Bioorg Med Chem Lett*, **2004**, 13, 3049-3053.
- [7] K. Gee-Hong, P. Catherine, D. Alan et al., *Bioorg Med Chem*, **2003**, 46, 4021.
- [8] A. Beauchard, H. Laborie, H. Rouillard, O. Lozach, Y. Ferandin, C. Guguen-Guillouzo, L. Meijer, T. Besson, V. Thiery, *Bioorg Med Chem*, **2001**, 17, 6257-6263.
- [9] C.A.Grimes, R.S. Jope, *Prog neurobiol*, **2001**, 65, 391.
- [10] H.Yong, H. Sung, L. Jung Hyane,P. Woo-Kyu, B. Du-Jong, K. Hun Yeong, C. Yong Seo, C. Hyunah, Ae Nim P, *Bioorg Med Chem*, **2008**,16, 2570-2578.
- [11] M. Clark, RD III.Cramer, *J Comput Chem*, **1989**, 10, 982-1012.
- [12] J. Gasteiger, M. Marsili, *Tetrahedron*, **1980**, 36, 3219-3228.